PHM2023 – 2023 Prognostics and Health Management Conference, Paris, France, 31 May – 02 June 2023

Robust structural control of onshore wind turbines using MR dampers

Peter Fakhry
Civil Engineering Department
The British University in Egypt
Cairo, Egypt
peter.fakhry@bue.edu.eg

Shady Salem
Civil Engineering Department
The British University in Egypt
Cairo, Egypt
shady.salem@bue.edu.eg

Mohammad O.Tokhi
Electric and Electronic Engineering Department
London South Bank University
London, UK
tokhim@lsbu.ac.uk

Duan Fang
Electric and Electronic Engineering Department
London South Bank University
London, UK
duanf@lsbu.ac.uk

***Abstract*—Nowadays, wind turbines are built in huge dimensions to cope with the high demand on renewable energy. Nevertheless, large and slender dimensions for blades and tower have fostered the problem of increased structural vibrations which led to undesirable deformations and destabilization in generator power production. Moreover, large dynamic responses for structural elements greatly reduces lifetime for these sensitive structures. During the past few decades, works on structural control of wind turbines have been carried out. However, their effectiveness is not significant in terms of reducing dynamic responses with minimum effort. This work introduces a Particle Swarm Optimized (PSO) semi-active controller which exploits Magnetorheological (MR) dampers to mitigate edgewise blade displacements. MR dampers are placed inside of each of the blades to effectively supress their dynamic vibrations. The proposed controller is tested on a benchmark 5-MW wind turbine for validity of application. The proposed approach showed significant reductions in blades peak and peak-to-peak displacements which promotes longevity of wind turbines and optimizing the wind turbine energy output.**

Keywords*— *wind turbines; magnetorheological dampers; particle swarm optimization; edgewise vibrations

I. Introduction

The installation of multi-megawatt turbines with huge tower and blade diameters has been made possible in recent years by the rising demand for wind energy [1]. The Cypress 6.0-164 wind turbine can produce up to 6.3 MW of power and has hub heights of 167 and 80 metres [2]. Yet, when subjected to environmental loads that destabilize their power production, such slender and enormous turbines are vulnerable to large dynamic responses and vibrations. Also, due to available space and increased wind intensities, the installation of offshore wind turbines in oceans has acquired widespread acceptability [3]. Indeed, when situated in very active wind zones, onshore wind turbines are vulnerable to extremely high wind intensities. As such, wind turbines subjected to high dynamic loading lose a significant range of their lifetime and need mitigation for power stabilization.

Structural control comes as a remedy to excessive structural deformations and damage. Throughout the past few decades, this discipline has undergone enormous advancements, particularly in relation to civil engineering [4], [5]. There are three operating modes for structural control: passive, active, and semi-active. When the control force is directly activated by the actuators, active control is obtained. On the other hand, semi-active controls work by adjusting the electric current or other settings of the control device, which changes the resistive force for the instrument being utilised. Semi-active control is used in this research because it offers the advantages of active control, such as high force capacity, while consuming much less power. Any synthesis between any of these three forms develops a hybrid control mode. Recently, structural control has been recently introduced to mitigate wind turbine structure deformation and dynamic responses whether onshore or offshore [1], [6]–[8].

The work of Fitzgerald et al. [9] is one of the earliest examples of structural control on wind turbines. The use of ATMDs in wind turbines to control the in-plane blade vibration responses was effectively adapted by the authors. They made use of a numerical model for the wind turbine that was based on the system's kinetic and potential energy. In order to arrive at the dynamic equation of the system based on their kinetic and potential energy, Euler Lagrange numerical model is adopted. In this work, two TMD modes, passive and active modes, were used, each set to 3% of the blade's in-plane frequency. The Linear Quadratic Regulator (LQR) control system was chosen for active control due to its optimality at calculating the necessary control force. Moreover, TMDs were positioned at 75% of the blade's length, measured from the hub, where the damper can have a 3m stroke. Four TMDs were used, three in each blade and one at the nacelle to supress tower responses. When compared to the uncontrolled blade responses, active control lowered the peak response of the blades by 18% in the peak response and 44% in the peak-to-peak response. Moreover, a reduction of 31% was achieved against the passively controlled blade regarding the peak-to-peak response.

A computational model for the wind turbine system was created by Staino and Basu [10] using the Lagrangian-Euler technique, taking into consideration the time-variant structural features and accounting for the fluctuating rotor speed brought on by system faults [11]. The implementation of an active tendon system mounted on a truss or frame structure inserted inside each blade was suggested by the authors. In order to manage the significant edgewise displacements caused in the blades by changes in rotor speed, they used a LQR to find the best active control forces generated in the tendons. Their modelling consequently revealed a discernible decline in the tip displacements for onshore wind turbines. A Tuned Liquid Passive Damper (TLD) was used by Zhang et al. [12] to reduce the side-to-side vibration of onshore wind turbines. They were inspired by the unfavourable outcome that results from the amalgamation of the drivetrain torsional moments and the lateral tower vibration. The latter causes oscillations in the power generated as well as instability in the generator torque. The authors have opted to use the Real-Time Hybrid Testing (RTHT) algorithm as a modelling technique for their system because TLDs are highly non-linear devices and the control force they create is governed by numerous parameters. Furthermore, a full-scale TLD was constructed and experimented to directly rely on its measured output in conjunction with a numerical 13-DOF wind turbine model. For a scaled-down 2-MW wind turbine, SD reductions ranged from 9% to 53% and from 2% to 49% in terms of peak response.

Caterino [13] investigated a semi-active control strategy on a wind turbine model scaled to 1/20 to see if it could reduce the dynamic structural reactions of onshore wind turbines in terms of tower base bending stresses and top displacement. MR dampers were installed at the foot of the tower to implement the semi-active control technique. Using a cylindrical hinge, two springs, and two MR dampers, the author introduced the idea of a variable restraint to withstand tower loads. The concept focused on identifying the structural requirements of the wind turbine, the bending loads at the tower base, and the top displacement. When MR dampers are included, the restraint can change its mechanical characteristics in response to tower motion, changing the structural requirements. Results demonstrated a decrease in the demand for bending stresses, which in some cases reached 64%, but at the expense of a 29% rise in top displacement.

Recent structural control attempts on wind turbines have been investigated, however the produced findings need to be more reliable in terms of suppressing dynamic responses while utilising the least amount of electricity possible.

This research proposes a unique optimised controller to limit excessive edgewise displacements of wind turbine blades employing Particle Swarm Optimized (PSO) semi-active control. Using MR dampers installed inside each blade with the possibility of considering various positions and/or numbers, semi-active control is accomplished. The effectiveness of the suggested method has been demonstrated in comparison to passively controlled system.

II. Wind Turbine Model

Based on the Euler-Lagrangian energy formulation, a multi-modal numerical model of a horizontal axis wind turbine (HAWT) is developed in this section. For a three-bladed HAWT with a tower fixed at the ground, a dynamic equation of motion is developed taking into consideration the dynamic coupling between the blades and tower. As shown in Fig. 1, the three blades are modelled as Euler-Bernoulli elastic beams with distributed mass $\mu_b(x)$ and elastic stiffness $EI(x)$ along its length. Blades are accounted for as cantilever beams fixed at the hub and the rotor is fixed with the tower where the latter is considered as a single Degree of Freedom (DOF) taking into consideration the tower modal mass M_T (as depicted in Fig. 1) in addition to the nacelle and hub masses. Indeed, in this paper, blades' dynamic responses are calculated from superposition of edgewise and flapwise components. Similarly, for the tower responses, they are expressed in the side-to-side and fore-aft senses.

The tower stiffness and damping terms have been considered in the developed numerical model in the side-to-side and fore-aft modes as K_T and C_T, respectively where C_T is the summation of the structural and aerodynamic damping. However the developed model accounts for variation in rotor speeds, the rotor is set to rotate at the rated speed Ω (rad/sec) and the azimuth angle $\Psi_j(t)$ (rad) of blade j is expressed in terms of time t as:

$$\Psi_j(t) = \Omega t + \frac{2\pi}{3}(j-1) \quad , j = 1,2,3 \tag{1}$$

The dynamic response of structural elements with distributed mass and elasticity is frequently described as a function of a generalised or a benchmark coordinate when they are considered as generalised single or multi DOF systems. In this work, the motion of the tower top/nacelle in the side-to-side and fore-aft directions, as well as the tip displacements of the blades in the edgewise and flapwise directions, are used as the generalised coordinate. In this work, the generalized coordinate is chosen to be the tip displacements of the blades in the edgewise and flapwise directions as well as the tower-top/nacelle motion in the side-to-side and fore-aft directions. Let N be the total number of DOFs for the HAWT and let k and i represent the respective plane of interest and the number of mode shape considered, respectively, then the generalized coordinates shall be expressed as:

$$\tilde{q}(t) = \{\tilde{q}_{1,in,1}(t)\ \tilde{q}_{1,out,1}(t)\ \tilde{q}_{2,in,1}(t)\ \tilde{q}_{2,k,i}(t) \ldots\ldots \tilde{q}_{j,k,i}(t)\ \tilde{q}_{4,k,i}(t)\}^{T}_{\in R^{N\times 1}} \tag{2}$$

Such that $k = \{in, out\}$, $i = 1,2, \ldots \ldots, n$ and n is the total number of modes considered for a specific plane of interest. Moreover, two generalized DOFs are considered for the tower in the side-to-side and fore-aft directions. The total number of DOFs for the HAWT numerical model is $N = 3n + 2 = 8$. As shown in Fig. 1, blade displacement at any given x position from the blade root is expressed as modal superposition of the generalized DOF for the blade as formulated in (3) and is given as:

$$u_{j,k}(x,t) = \sum_{i=1}^{n} \phi_{i,k}(x)\tilde{q}_{j,k}(t) \tag{3}$$

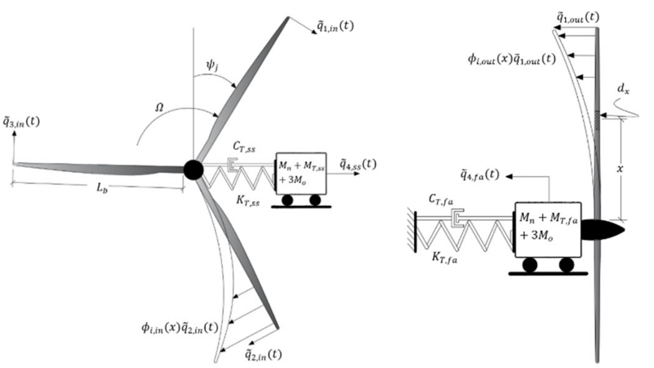

Fig. 1. Numerical model and generalized DOF definition for wind turbine

For forced vibration systems, the Euler-Lagrange equation is expressed in terms of partial derivatives of the Lagrangian L with respect to the generalized coordinate and its time derivative as:

$$\frac{d}{dt}\left(\frac{\partial L}{\partial \dot{\tilde{q}}}\right)=\left(\frac{\partial L}{\partial \tilde{q}}\right)+Q_{ext}+\Gamma \mathbf{F}_D \tag{4}$$

where Q_{ext} is the aerodynamic and gravitational loads acting on the HAWT blades and tower, respectively and $\in R^{N\times 1}$ the Lagrangian L is the difference in kinetic T and potential V energies of the system as:

$$L = T - V \tag{5}$$

A. HAWT Kinetic Energy

The total kinetic energy of the system can be formulated as a superposition of its component's kinetic energies as shown in (6).

$$T = \frac{1}{2}\left[\sum_{j=1}^{3}\left[\int_0^{L_b}\mu_b(x)v_j(x,t)^2dx\right]+\left[\int_0^{L_T}\mu_T(z)v_4(z,t)^2dz\right]+ (M_{hub}+M_{nac})v_4(L_T,t)^2\right] \tag{6}$$

where v_j is the total velocity in edgewise and flapwise directions of an incremental part along the blade j located at distance x from the hub at time t. Similarly, v_4 is the total velocity of in the side-to-side and fore-aft directions of an incremental segment along the tower located at distance z from the ground at time t.

B. HAWT Potential Energy

Potential energy of the system arises from elastic stiffness of the blades in bending K_e, geometrical or centrifugal stiffening K_C of the blades that arises from tensile forces induced due to rotation, gravitational stiffening K_g arising from gravity forces acting on the blades and tower/nacelle potential energy. The total potential energy for the HAWT system is given by:

$$V = \frac{1}{2}\sum_{j=1}^{3}\left[\sum_{k=in}^{out}\sum_{i=1}^{n}\left(K_{e,kk',ii'}+K_{c,k,ii'}+K_{g,j,k,ii'}\right)\tilde{q}_{j,k,i}(t)\tilde{q}_{j,k',i'}(t)\right]+ \frac{1}{2}\sum_{k=ss}^{fa}\sum_{i=1}^{n}K_{T,k,ii'}\tilde{q}_{4,k,i}(t)\,\tilde{q}_{4,k,i'}(t) \tag{7}$$

such that k' is also the plane of interest (i.e., in or out) however can take a different value than k. The same goes for i' which loops through the plane of interest order but can also take different value than i.

$$K_{c,k,ii'}(x) = \Omega^2\int_0^{L_b}\left[\int_x^{L_b}\mu_b(\varrho)\varrho\, d\sigma\right]\left(\phi_{i,k}(x)'\phi_{i',k}(x)'\right)\,dx \tag{8}$$

$$K_{g,j,k,ii'}(x) = -g\cos\left(\psi_j(t)\right)\int_0^{L_b}\left[\int_x^{L_b}\mu_b(\varrho)\, d\sigma\right]\left(\phi_{i,k}(x)'\phi_{i',k}(x)'\right)\,dx \tag{9}$$

$$K_{e,kk',ii'}(x) = \int_0^{L_b}EI_{kk'}(x)''\phi_{i,k}(x)''\phi_{i',k'}(x)''\,dx \tag{10}$$

where ϱ is a distance from the distance x along the blade to the full length of the blade and $\phi_{i,k}(x)'$ and $\phi_{i,k}(x)''$ are the first order and second order derivatives with respect to x, respectively.

C. External Loads

From (4), the Euler-Lagrange equation, Q_{ext} and F_D are the external generalized applied loads consisting of aerodynamic and gravitational loads and MR damper forces such that:

$$Q_{ext} = Q_a + Q_g \tag{11}$$

such that Q_a is a vector of applied wind loads on the blades and nacelle in the in-plane and out-of-plane directions and Q_g is the gravitational loads due to the blades' own weight considering blades rotation. Aerodynamic and gravitational loads are applied as modal loads acting along the generalized corresponding DOF which is eventually the blade tip as:

$$Q_{a,j,ki}(t) = \int_0^{L_b}\phi_{i,k}(x)l_{j,k}(x,t)\,dx \tag{12}$$

where $l_{j,k}$ is the respective aerodynamic load on blade j in the edgewise (tangential) or the flapwise (normal) direction calculated from the Blade Element Momentum (BEM) theory algorithm while the loads that act on the nacelle are given by:

$$Q_{a,4,ss}(t) = \sum_{j=1}^{3}\int_0^{L_b}l_{j,in}(x,t)\cos(\psi_j(t))\,dx \tag{13}$$

$$Q_{a,4,fa}(t) = \sum_{j=1}^{3}\int_0^{L_b}l_{j,out}(x,t)\,dx \tag{14}$$

where $Q_{a,4,ss}(t)$ and $Q_{a,4,fa}(t)$ are the nacelle/tower top aerodynamic loads acting in the side-to-side and fore-aft directions, respectively. As for the MR damper forces, they are applied on blades as modal loads as well such that:

$$F_D = \begin{Bmatrix} f_{d,1,k} \\ f_{d,2,k} \\ f_{d,3,k} \end{Bmatrix}_{\in R^{3\times 1}} \tag{15}$$

$$f_{d,j,k} = \int_0^{L_d}\phi_{i,k}(x)\,dx\; p_{j,k}(t) \tag{16}$$

Such that $p_{j,k}$ is the commanded force by the MR damper in direction k and is installed in blade j and L_d is the distance from the blade root to the damper's location the blade length. As for the gravitational load, it is given by:

$$Q_{g,j,in,i}(t) = \int_0^{L_b} \mu_b(x)\phi_{i,in}(x)dx \sin(\psi_j(t)) \tag{17}$$

where $Q_{g,j,in,i}$ is the generalized gravity load acting on the blade j in the i^{th} in-plane mode. Indeed, no gravity loads act on the nacelle in any direction as it is transmitted to the ground via the tower as well as no gravity loads act in the blade's out-of-plane direction.

III. MR DAMPER NUMERICAL MODEL

The MR damper is a promising actuator for structural control purposes that has attracted a lot of interest over the past few decades. Dynamic responses mitigation of tall structures has made substantial use of these semi-active control systems, as has the mitigation of dynamic reactions in wind turbines and bridges [14]–[16]. Moreover, the use of MR dampers has been incorporated into wind turbine structural control to reduce dynamic responses of various structural parts [13], [17]–[19]. A 5000 N maximum force damper is employed in this paper. Several mechanical models have been described in literature that, when given a precise voltage or current as an input, can forecast the force generated by MR dampers. The numerical model created by Spencer et al. is a common one that can forecast the MR damper force [20].

Since this model takes into account the impacts of low velocities and the accumulator stiffness contained in the damper, it has been widely used in structural control works utilizing MR dampers. The improved Bouc-Wen mechanical model is schematically represented in Fig. 2 with the force F being the linear combination of the spring stiffness k_1 force and the dashpot c_1 force, which are provided as:

$$F = c_1\dot{y} + k_1(x\text{-}x_0) \tag{18}$$

such that:

$$\dot{y} = \frac{1}{(c_0+c_1)}[\alpha z+c_0\dot{x}+k_0(x\text{-}y)] \tag{19}$$

and the evolutionary variable $\dot{z}$ is governed by:

$$\dot{z} = -\gamma|\dot{x}\text{-}\dot{y}|z|z|^{n-1} - \beta(\dot{x}\text{-}\dot{y})|z|^n + A(\dot{x}\text{-}\dot{y}) \tag{20}$$

where x is the displacement of the damper piston, y is the displacement of the dashpot c_1. γ, n, β, A are the parameters regarding the Bouc-Wen hysteresis loop where they can control the nonlinear behavior of the yielding element [20].

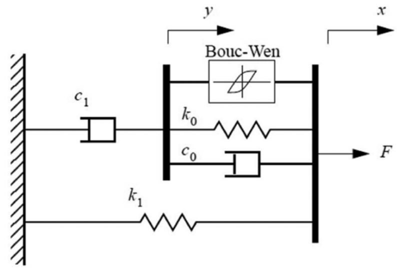

Fig. 2. Modified Bouc-Wen MR schematic model

The modified Bouc-Wen model also accounts for the change of the hysteresis nonlinear loop in response to the applied current as:

$$\begin{aligned}\alpha(u) &= \alpha_a+\alpha_b u\\ c_0(u) &= c_{0a}+c_{0b}u\\ c_1(u) &= c_{1a}+c_{1b}u\end{aligned} \tag{21}$$

such that u is the output of a first order filter that accounts for the dynamics introduced to the system for the MR fluid to reach rheological equilibrium [20] and is governed by:

$$\dot{u} = -\eta(u\text{-}v) \tag{22}$$

where v is the voltage applied to the current driver to the damper and $1/\eta$ is the time constant of this first order filter.

IV. SIMULATION RESULTS AND DISCUSIION

A. Model Description

Numerical simulations using MATLAB have been done to show the effectiveness of the proposed optimised LQR semi-active controller. For numerical simulation and testing in this context, the benchmark 5-MW baseline HAWT created by Jonkman et al. has been used [21]. The numerical model created for simulation accounts for the fundamental edgewise and flapwise modes for blades as well as the fundamental side-to-side and fore-aft directions of the tower, resulting in an 8-DOF system. It is to be noted that all simulations are carried at the rated rotor speed $\Omega = 12.1\ rpm$. In order to compute the appropriate shape functions (in-plane and out-of-plane) for the blade in hand needed for generalized solutions, BModes tool has been used [22].

B. Controller Design with MR dampers Configuration

PSO has been implemented to design a smart controller capable of controlling edgewise blade displacements effectively. Referring to Fig. 3, simulations took place such that five dampers are used to suppress edgewise vibrations, named PS-5. Furthermore, L_d is taken to be equal to $10\ m$ so that MR dampers are connected between the blade tip and at $51.5\ m$ from the hub. The PSO semi-active controller is optimized towards a goal fitness function as the average of the MSE of tip displacements for the three blades. For PS-5 controller, swarm size is set to 6 particles, no. of iterations is determined after the optimizer reaches the minimum goal value with maximum number of stall iterations 50 limited to 100.

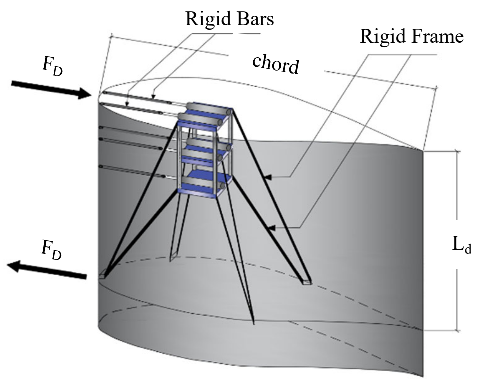

Fig. 3. MR dampers within vicinity of airfoil

C. Results

The 5-MW benchmark HAWT was tested for case PS-5. As noted from Fig. 4, blade tip displacement time domain plot between the proposed semi-active and passive controllers, that the PSO control algorithm has mitigated the dynamic response significantly. Time domain results are plotted for blade 2 and blade 3 in Fig. 5 and Fig. 6 respectively which witnessed a similar behaviour as well. Reductions in blade edgewise peak displacement for blade 1 exceeded 80% when using PS-5 while only 69% using a passive controller. The proposed controller targets as well stabilization of power output produced by the wind turbine that may happen from abrupt increases in rotor speed arising from excessive blade displacements.

Peak-to-peak displacement represents a crucial factor to express fatigue stresses induced on wind turbine blades and thus their mitigation is indeed an important matter specially to promote blades longevity. Similar results were achieved regarding reductions in the peak-to-peak displacement of blade 1 reaching 69% for the passive controller and a 77% using the proposed controller.

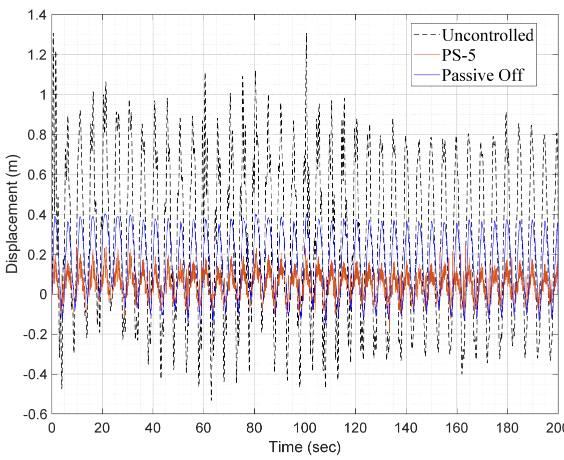

Fig. 4. Blade 1 tip displacement for semi-active (PS-5) and passive off controllers

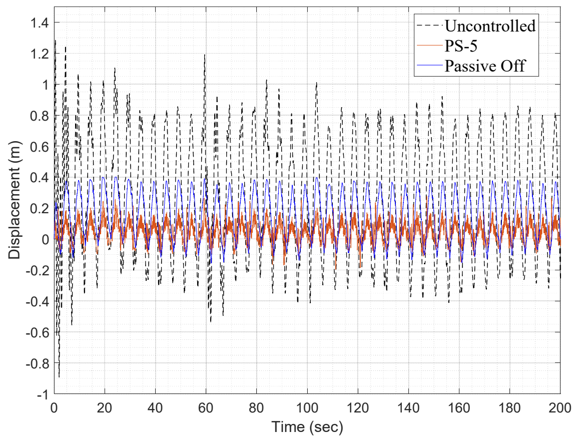

Fig. 5. Blade 2 tip displacement for semi-active (PS-5) and passive off controllers

Fig. 7 shows how the proposed controller performed better than passive control in reducing the peak tip displacement while Fig. 8 also represents the effectiveness of PS-5 controller in reducing peak-to-peak displacement over the passive controller.

As noted from the previous simulation results, the proposed semi-active controller incorporating MR dampers has significantly improved the blades' performance. Indeed, reducing dynamic responses for blades greatly impacts the structural design for blades in specific and HAWTs in general.

V. Conclusion

In this work, a new method of mitigating edgewise blade vibrations for HAWTs is developed. For the first time, PSO has been integrated into a semi-active control scheme by optimizing a conventional LQR controller to achieve the best dynamic suppression with minimum actuation effort. A 5-MW benchmark HAWT is used for testing and simulation of the proposed controller.

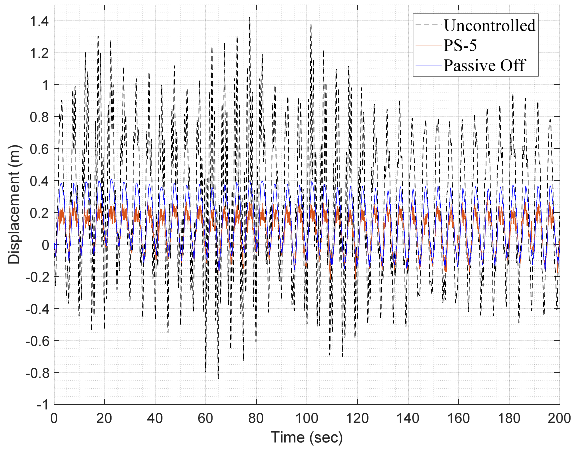

Fig. 6. Blade 3 tip displacement for semi-active (PS-5) and passive off controllers

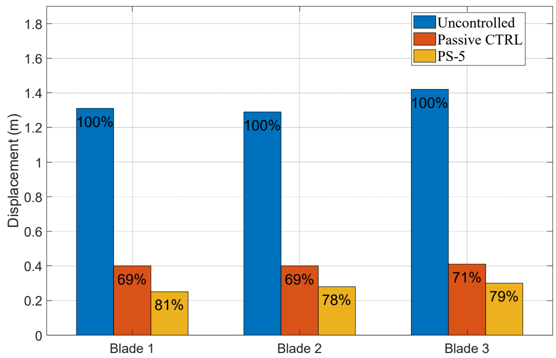

Fig. 7. Bar chart comparing reductions of peak displacement for different controllers

Besides MR dampers compatibility to fit within the airfoil's vicinity, the proposed 5-damper configuration does not require any superimposed structure to support dampers in position and spanning to the rotor hub. Thus, it is an efficient and yet well performing configuration-controller system. Simulation results show the outperforming of the proposed controller over passive ones. Indeed, peak displacement for blades was reduced by over 80% which eliminates any destabilization of power production that may occur due to undesirable displacements. Moreover, peak-to-peak displacement, which is an important measure of fatigue, also witnessed a reduction of about 78%. In addition, results obtained promote longevity of wind turbine blades and to a more robust structural design.

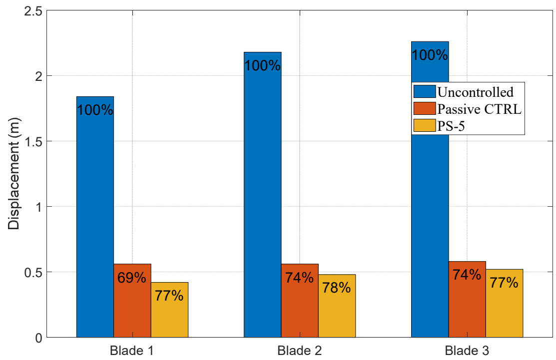

Fig. 8. Bar chart comparing reductions of peak-to-peak displacement for different controllers

References

[1] H. Zuo, K. Bi, and H. Hao, "A state-of-the-art review on the vibration mitigation of wind turbines," *Renew. Sustain. Energy Rev.*, vol. 121, no. July 2019, p. 109710, 2020, doi: 10.1016/j.rser.2020.109710.

[2] "GE's Most Powerful Onshore Wind Turbine Gets Even More Powerful." https://www.ge.com/news/press-releases/ge-most-powerful-onshore-wind-turbine-gets-even-more-powerful (accessed Feb. 12, 2023).

[3] M. Karimirad, *Offshore Energy Structures For Wind Power, Wave Energy and Hybrid Marine Platforms*. Springer, 2014. doi: 10.1007/978-3-319-12175-8.

[4] J. P. Ou and H. Li, "the State-of-the-Art and Practice of Structural Control of Civil Structures for Hazard Mitigation in Mainland China," *Iitk.Ac.in*, 2008, [Online]. Available: http://www.iitk.ac.in/nicee/wcee/article/14_S24-015.PDF

[5] T. E. Saaed, G. Nikolakopoulos, J. E. Jonasson, and H. Hedlund, "A state-of-the-art review of structural control systems," *JVC/Journal Vib. Control*, vol. 21, no. 5, pp. 919–937, 2015, doi: 10.1177/1077546313478294.

[6] J. G. Njiri and D. Söffker, "State-of-the-art in wind turbine control: Trends and challenges," *Renew. Sustain. Energy Rev.*, vol. 60, pp. 377–393, 2016, doi: 10.1016/j.rser.2016.01.110.

[7] Y. Yang, B. Musa, M.-N. Yue, and C. Li, "A Review on the State-of-the-Art of Seismic Analysis of Wind Turbines," *Reneng Dongli Gongcheng/Journal Eng. Therm. Energy Power*, vol. 34, no. 9, pp. 14–23 and 56–23 56, 2019, doi: 10.16146/j.cnki.rndlgc.2019.09.002.

[8] F. Xie and A. M. Aly, "Structural control and vibration issues in wind turbines: A review," *Eng. Struct.*, vol. 210, no. September 2019, p. 110087, 2020, doi: 10.1016/j.engstruct.2019.110087.

[9] B. Fitzgerald, B. Basu, and S. R. K. Nielsen, "Active tuned mass dampers for control of in-plane vibrations of wind turbine blades," *Struct. Control Heal. Monit.*, vol. 20, no. 12, pp. 1377–1396, 2013, doi: 10.1002/stc.1524.

[10] A. Staino, B. Basu, and S. R. K. Nielsen, "Actuator control of edgewise vibrations in wind turbine blades," *J. Sound Vib.*, vol. 331, no. 6, pp. 1233–1256, 2012, doi: 10.1016/j.jsv.2011.11.003.

[11] A. Staino and B. Basu, "Dynamics and control of vibrations in wind turbines with variable rotor speed," *Eng. Struct.*, vol. 56, pp. 58–67, 2013, doi: 10.1016/j.engstruct.2013.03.014.

[12] Z. Zhang, A. Staino, B. Basu, and S. R. K. Nielsen, "Performance evaluation of full-scale tuned liquid dampers (TLDs) for vibration control of large wind turbines using real-time hybrid testing," *Eng. Struct.*, vol. 126, pp. 417–431, Nov. 2016, doi: 10.1016/j.engstruct.2016.07.008.

[13] N. Caterino, "Semi-active control of a wind turbine via magnetorheological dampers," *J. Sound Vib.*, vol. 345, pp. 1–17, 2015, doi: 10.1016/j.jsv.2015.01.022.

[14] P. Fakhry, A. A. Torky, and Y. F. Rashed, "Optimized Seismic Response Control of Coupled FEM-BEM High-Rise Structural Models Using Magnetorheological Dampers," *J. Earthq. Eng.*, vol. 26, no. 15, pp. 1–28, 2021, doi: 10.1080/13632469.2021.1987355.

[15] M. Braz-César and R. Barros, "Optimal control of a plan asymmetric structure using magnetorheological dampers," *Arch. Appl. Mech.*, vol. 87, no. 5, pp. 893–904, 2017, doi: 10.1007/s00419-016-1191-z.

[16] S. Jothinathan, S. Kashyap, D. Kumar, and N. Saha, "Response control of fixed offshore structure with wind turbine using MR damper," in *Oceans Conference Record (IEEE)*, 2022. doi: 10.1109/OCEANSChennai45887.2022.9775436.

[17] J. Chen, C. Yuan, J. Li, and Q. Xu, "Semi-active fuzzy control of edgewise vibrations in wind turbine blades under extreme wind," *J. Wind Eng. Ind. Aerodyn.*, vol. 147, pp. 251–261, 2015, doi: 10.1016/j.jweia.2015.10.012.

[18] P. Martynowicz, "Control of a magnetorheological tuned vibration absorber for wind turbine application utilising the refined force tracking algorithm," *J. Low Freq. Noise Vib. Act. Control*, vol. 36, no. 4, pp. 339–353, 2017, doi: 10.1177/1461348417744299.

[19] C. Sun, "Semi-active control of monopile offshore wind turbines under multi-hazards," *Mech. Syst. Signal Process.*, vol. 99, pp. 285–305, 2018, doi: 10.1016/j.ymssp.2017.06.016.

[20] B. F. J. Spencer, S. J. Dyke, M. K. Sain, and J. D. Carlson, "Phenomenological Model for Magnetorheological Dampers," *J. Eng. Mech.*, vol. 123, no. 3, pp. 230–238, 1997, doi: 10.1061/(ASCE)0733-9399(1997)123:3(230).

[21] J. Jonkman, S. Butterfield, W. Musial, and G. Scott, "Definition of a 5-MW reference wind turbine for offshore system development," 2009. [Online]. Available: http://tethys-development.pnnl.gov/sites/default/files/publications/Jonkman_et_al_2009.pdf

[22] G. S. Bir, "User's Guide to BModes," *Natl. Renew. Energy Lab.*, no. September, 2007, [Online]. Available: https://nwtc.nrel.gov/system/files/BModes.pdf